9 December 1994

ELSEVIER

Chemical Physics Letters 230 (1994) 495–500

CHEMICAL PHYSICS LETTERS

Molecular dynamics simulations of keV particle bombardment. Correlation of intact molecular ejection with adsorbate size

Ramona S. Taylor [1], Barbara J. Garrison

Department of Chemistry, 152 Davey Laboratory, Penn State University, University Park, PA 16802, USA

Received 1 August 1994; in final form 26 September 1994

Abstract

Molecular dynamics simulations employing a reactive many-body potential of the keV particle bombardment of small hydrocarbon molecules adsorbed on a metal surface have been performed. The simulations predict the occurrence of considerable lateral motion of particles in the region right above the surface. For adsorbates such as CH_x, dominant ejected species are an H atom or the intact adsorbate as there are only two unique bonds to sever. Molecules that extend further above the surfaces are exposed to more collisions from laterally moving particles and consequently there is more fragmentation and the dominant ejected species is usually not the original adsorbate.

1. Introduction

High-energy particle bombardment is a potentially powerful method for probing the intermediates of complex catalytic reactions [1–7]. With secondary ion mass spectrometry (SIMS) and temperature programmed desorption, for example, Kaminsky and coworkers were able to identify the intermediates in the formation of CH_4 via the methanation reaction of CO and H_2 over nickel as being methylidyne (CH), methylene (CH_2), and methyl (CH_3) from the direct observation of each of these species in the SIMS spectrum [6]. In other investigations, however, peaks corresponding to the most probable intermediate are not found [3–5,7]. For instance, although polypylidyne (C_3H_5) is agreed to be the dominant product resulting from the hydrogenation of propylene over Pt, it is not observed in the SIMS spectrum of this system [3–5]. In these examples, spectral assignments must be inferred from related information and cannot be deduced directly from the experimental SIMS spectrum.

Molecular dynamics computer simulations offer a powerful approach for disentangling the various factors which lead to intact ejection of reaction intermediates [8–15]. Accurate calculations of this sort are now feasible because of the recent development of many-body potential functions which describe the forces among simple organic molecules [16,17] and among metal atoms [18–21] along with a prescription for merging them together [22–24]. Specifically we have modeled the 500 eV Ar bombardment of small $CH_{x\,(x=0-3)}$ adsorbates on Pt{111} as shown in Fig. 1a as well as the larger $C_yH_{2y-1\,(y=2-5)}$ adsorbates shown in Fig. 1b. In this communication we describe the important mechanistic differences for ejection between these two groups of adsorbates. Lateral motion of fragments of the overlayer is the key factor identified from the simulations that leads to the experimental observations. The longer hydrocarbons

[1] Present address: Molecular Science Research Center, Pacific Northwest Laboratory, Richland, WA 99352, USA.

SSDI 0009-2614(94)01196-6

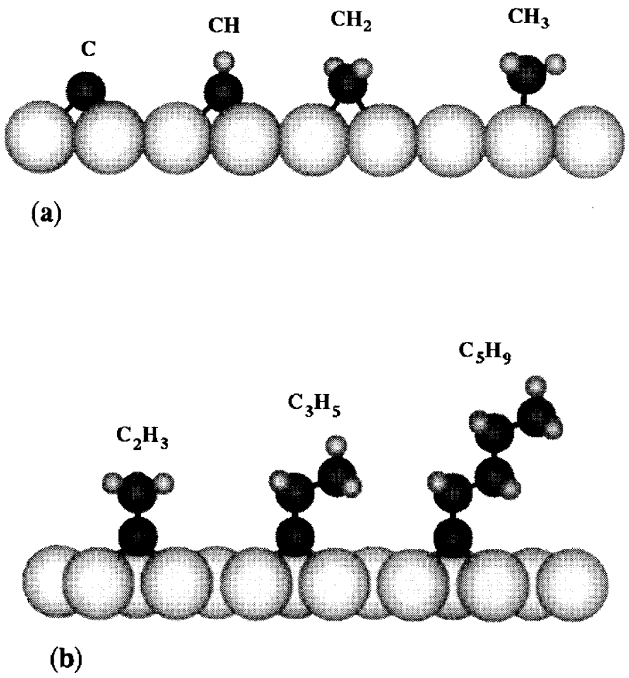

Fig. 1. Equilibrium binding site configurations of (a) $CH_{x\,(x=0-3)}$ and (b) $C_yH_{2y-1\,(y=2-5)}$ hydrocarbons chemisorbed on the {111} surface of Pt. The light gray spheres represent Pt atoms, the dark gray spheres represent C atoms and the small medium gray spheres represent H atoms.

have more C–C bonds that can be readily severed by the laterally moving particles.

2. Method

The 500 eV Ar bombardment of p(2×2) films of C, CH, CH_2, CH_3, C_2H_3, C_3H_5, and C_5H_9 chemisorbed on the {111} face of platinum are modeled via molecular dynamics (MD) computer simulations. The classical MD scheme has been described in detail elsewhere [8–15]. The forces among the various atoms are calculated using a carefully selected blend of empirical potential energy functions. The Ar–Pt, Ar–C, and Ar–H interactions are described using a purely repulsive Molière pair-wise potential energy function [25]. For the remainder of the particles, both the repulsive and attractive interactions among the particles are included. The Pt–Pt interactions are described by an attractive, many-body potential function based upon the embedded atom method (EAM) [18–20]. The EAM Pt potential is chosen as energy and angular distributions calculated from MD simulations of the high energy bombardment of other fcc metals using the EAM potentials compare well with the corresponding experimental observations [21,26].

The C–C, C–H, and H–H interactions are described with a reactive many-body potential energy function developed by Brenner [16,17] which not only describes the energetics of bulk diamond and graphite, but also those of a wide array of small hydrocarbon molecules, such as C_2H_4, C_2H_6, and C_6H_6, and radicals, such as $\cdot CH_3$ and $\cdot C_2H_5$. This potential has been successfully applied to MD simulations of a variety of chemical reactions including hydrogen abstraction from hydrogen terminated diamond surfaces [27,28], the compression of fullerenes between two graphite sheets [29], and the nonequilibrium tribochemical reactions of diamond surfaces [30–32]. The Pt–H interactions are described with a Lennard-Jones potential and the Pt–C interactions are described via a potential energy function that consists of a Lennard-Jones pair-wise component and a many-body component specifically designed to work in conjunction with Brenner's hydrocarbon potential [23,24]. Due to this many-body component, the three-fold site is not the lowest energy binding site for all adsorbates as would be the case with a simple pair-wise potential. Instead, each adsorbate binds in the site which best preserves the sp^3 coordination of the binding C atom. Thus, methylidyne, CH, binds in the three-fold site; methylene, CH_2, bind in the two-fold bridge site; and methyl, CH_3, binds in the atop site. The binding energies of these adsorbates to the substrate are 7.01, 5.67, and 2.86 eV, respectively. The binding energy to the substrate of both the C_2H_3 and C_3H_5 adsorbate is 7.35 eV which is well within the experimental range of 6.9 to 8.5 eV [33,34]. As this energy is relatively large compared to the C–C and C–H bond strengths we chose to decrease the Lennard-Jones well depth of the Pt–C potential such that the binding energy of each C_5H_9 adsorbate is only 2.70 eV.

The crystal sizes are chosen to be large enough such that the main dynamical effects of the collisional impact are retained. For C, CH, CH_2 and CH_3 adsorbates the Pt substrate is approximated by a finite microcrystallite containing 1260 Pt atoms arranged in seven layers. Each hydrocarbon is then placed in its

lowest energy position in a p(2×2) configuration. For both the C and CH films, 39 adsorbates are chemisorbed in the hcp three-fold sites. For the methylene film, 35 CH_2 adsorbates are placed in the two-fold bridge sites, and for the CH_3 film, 39 adsorbates are placed in the atop sites. The bombardment of the larger hydrocarbon chains result in more reaction than the smaller C_1 adsorbates discussed above and thus require a larger Pt substrate to contain the effects of the collisional impact. The binding carbon atoms in C_2H_3, C_3H_5, and C_5H_9 all require three Pt neighbors to be fully coordinated, thus each molecule is placed in the fcc hollow site. (Due to the short-ranged nature of the Pt–C potential, the binding energies of hydrocarbon films adsorbed in both the hcp and the fcc three-fold sites are equivalent.) The Pt–C_2H_3 system is modeled by a microcrystallite containing 1512 Pt atoms arranged in seven layers and a C_2H_3 film consisting of 45 adsorbates. The Pt–C_3H_5 and Pt–C_5H_9 systems are both modeled with a crystallite containing 1996 Pt atoms arranged in six layers and a film consisting of 77 adsorbates. In all simulations, open boundary conditions are used [8–10].

With the exception of the C_5H_9 film, no less than 500 trajectories were run for each of the films. For C_5H_9, each trajectory requires between 8 to 12 h of CPU time on one node of an IBM SP1 computer and thus only 50 trajectories were calculated for this system. Each trajectory is terminated when the total energy of any atom remaining in the solid falls below the level where any further ejection can take place.

3. Results and discussion

Calculated mass distributions are determined by counting the neutral species which exist 1–2 ps after the bombardment event. We have not attempted to account for experimental factors of ionization probability, ion stability or possible further fragmentation of the larger clusters during the μs flight to the detector. For convenience the calculated distributions are plotted as 'mass spectra'. This graphical representation provides a starting point for identifying dominant results for mechanistic analysis and for comparisons to experimental data.

Comparison of overlayers: The calculated results for normal incident Ar atom bombardment of p(2×2) films of the smaller CH_x hydrocarbons and the larger C_yH_{2y-1} hydrocarbons are shown in Figs. 2 and 3, respectively. With the exception of the CH results shown in Fig. 2b, the largest CH_x peak given in Fig. 2 is that of the intact adsorbate, or the parent species. In contrast, the composition of the most probable species shown in Fig. 3 for C_2H_3, C_3H_5, and C_5H_9 consists of some portion of the original adsorbate.

An analysis of atomic motions in these simulations and others [12–15,35] shows that for chemisorbed species to be ejected intact, a collision near the attachment point to the surface must occur. Moreover, there must be an escape route for the molecule. The whole process is easier for the small CH_x adsorbates. As the adsorbate length increases the path of particles

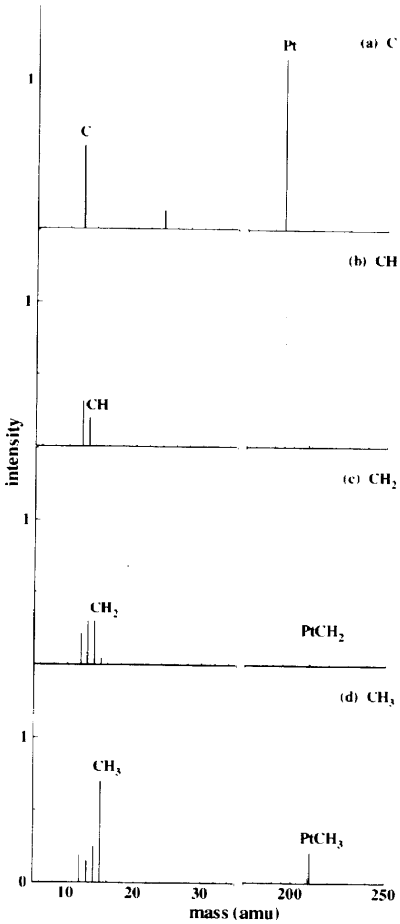

Fig. 2. Calculated results for 500 eV Ar bombardment of various CH_x overlayers chemisorbed on Pt{111}: (a) C, (b) CH, (c) CH_2, (d) CH_3. The H and H_2 peaks are not shown. The intensity scale is the particle yield and thus all frames in Figs. 2 and 3 are directly comparable.

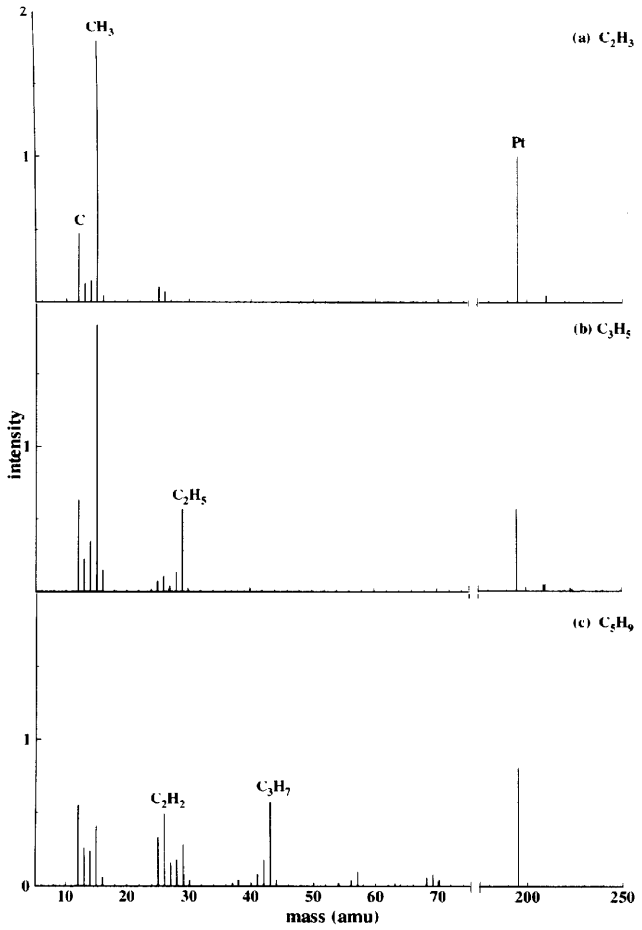

Fig. 3. Calculated results for the 500 eV Ar bombardment of various C_yH_{2y-1} overlayers chemisorbed on Pt{111}: (a) C_2H_3, (b) C_3H_5, (c) C_5H_9. The H and H_2 peaks are not shown.

trying to escape is obstructed and simultaneously there is a chance of fragmentation of other molecules. In fact, there is considerable lateral motion of organic fragments within the overlayer that can cause subsequent fragmentation.

Since relatively little fragmentation is found for the smaller C_1 adsorbates, it is relatively straightforward to determine the reaction intermediates on the surface from the SIMS spectra. Even in the case of CH, which exhibits more C than CH ejection in the calculation, the largest intensity seen experimentally [6] would be that of CH due to the higher ionization potential of C relative to CH (11.26 versus 10.64 eV). A simple model for relative ion intensities predicts that the ratio of intensities for two species should be proportional to the exponential of the difference in ionization potentials divided by a constant which typically has a value of 0.3–0.5 eV [2]. This correction factor would reduce the relative amount of C^+ by a factor of 3–10 as compared to the CH^+ intensity.

Sizeable $PtCH_2$ and $PtCH_3$ intensities are predicted for the methylene and methyl overlayers as shown in Figs. 2c and 2d. For the larger hydrocarbon overlayers, there is less Pt ejected and consequently fewer $PtCH_x$ species. Moreover the CH_x species generally originate at the top of the hydrocarbon chain, several angstroms above the starting position of the Pt atom. The probability for reaction thus is low. At this stage the specifics of the potential surfaces including the binding energies for the gas phase $PtCH_x$ species are unknown. As a reference point the interaction potential that we are using has a binding energy of 2.3 eV between the Pt and hydrocarbon species. A more quantitative discussion of these species requires more information.

Propylidyne: The C_3H_5 results, shown in Fig. 3b, are quite different from those reported by White and co-workers [3–5]. This molecule is believed to be the dominant intermediate through which the Pt catalyzed dehydrogenation of propene, $CH_3CH{=}CH_2$, proceeds [3–5,7,36]. Its proposed structure shown in Fig. 1b is analogous to that of C_2H_3. Consequently, one might expect a strong C_2H_5 peak. Nevertheless, the experimental mass spectrum is dominated by CH_3^+ and $C_2H_3^+$ peaks [3–5]. Our calculated result exhibits intense CH_3 and C_2H_5 features. Investigations using SIMS performed in conjunction with electron energy loss spectroscopy suggest that C_3H_5 adsorbed on Ru upon heating undergoes further decomposition to yield C_2H_3 [7]. Upon inspection of the calculated C_2H_3 result shown in Fig. 3a, this does not account for the increased C_2H_3 signal since very little intact C_2H_3 is actually detected in the bombardment of a pure C_2H_3 film.

The difference between the dominant species in the calculation and the experiment could depend on several factors. First, the C_2H_5 could decompose before being detected. The fragmentation channel of neutral C_2H_5 should proceed through the highly stable H_2CCH_2 species. SIMS experiments measure ejected

[2] This parameter is often expressed in terms of temperature although most researchers in the field have tried to avoid the word temperature as there does not appear to be experimental justification for assuming a thermal equilibrium.

ions, whereas these calculations only determine the yield of ejected neutral species. The energy cost to form $C_2H_3^+$ from C_2H_4 is almost 11 eV and consequently probably does not occur [37]. Second, the ejected C_2H_5 could actually be an ion in which case decomposition to $C_2H_3^+$ and H_2 is a real possibility. Finally, the structure on the Pt{111} surface is not propylidyne as shown in Fig. 1b and is, in fact, a structure that is consistent with a large $C_2H_3^+$ ion intensity. The EELS and TPD data, however, are consistent with a propylidyne structure [3–5] and we do not have a suggestion for a different structure. The ultimate resolution of this question awaits incorporation of electronic effects such as ionization into the calculations.

Pentylidyne: It is interesting to note that very little C_4 species are predicted to occur in the C_5H_9 simulations. As shown in Fig. 1b, C_5H_9 has two bond axes perpendicular to the Pt surface. If the linker C atom adjacent to the Pt surface is identified as C^1, then the first perpendicular axis runs through the C^1–C^2 bond and the second runs through the C^3–C^4 bond. Frequently, the ejection of a C_5H_9 adsorbate is initiated by a bump from an ejecting Pt atom or C_nH_m fragment. If the collision occurs toward the top of the C_5H_9 adsorbate, a fragment of the adsorbate usually ejects. If the collision occurs toward the bottom of the adsorbate, however, a C_3H_7 species results. In this latter case, the initial impact moves the C^1–C^2 axis into and across the C^3–C^4 axis causing the C^3 atom to coil up towards the C^4–C^5 bond. The recoil caused by the string of the momentary C^3–C^4–C^5 ring leads to the scission of the C^2–C^3 bond. This scenario is finished within less than 50 fs and is thus quicker than any possible momentum transfer between the lower and upper C atoms. The implications of this scenario are not obvious and will be the object of further investigation.

4. Conclusions

Molecular dynamics simulations using a blend of reactive, empirical potential energy functions show that the ejection processes of small CH_x adsorbates to be different from those of larger $C_yH_{2y-1\ (y=2-5)}$ adsorbates. Intact ejection is promoted by collisions that sever the adsorbate–substrate bond followed by removal of the particle into the vacuum. First, this whole process is easier for the smaller adsorbates as the Ar more often directly hits the metal substrate and also there are no obstructions to ejection. Second, in the longer chains there are more C–C bonds that are broken by lateral motion of pieces of the overlayer. As an ejecting adsorbate or fragment moves across the surface it can collide with and cause the fragmentation of even more adsorbates. For the small adsorbates this pathway, however, either ejects the whole adsorbate or knocks off an H atom.

In disagreement with the experimental findings for the 500 eV Ar bombardment of C_3H_5 adsorbed on Pt{111}, these calculations predict the existence of a large C_2H_5 peak instead of a large $C_2H_3^+$ peak. Resolution of this discrepancy awaits more advanced theoretical models.

The results presented here are collected from massive molecular dynamics calculations aimed at describing unknown *reactive* dynamics among a multitude of atoms in a complex environment. The major strength of this approach is that key mechanistic steps such as the lateral motion of organic fragments originally not recognized can be readily identified. As noted above, there are still shortcomings in our model. A decade ago [12–15] however, it was not possible to examine reactions as complex as those presented here, and we believe it is only a matter of time before other physics such as electronic effects will be included in simulations. Moreover, the atomistic predictions achieved so far are well-suited to combine with theories of electronic excitation and unimolecular decay.

Acknowledgement

The financial support of the National Science Foundation and the IBM Selected University Research program is gratefully acknowledged. We thank Nicholas Winograd, Donald W. Brenner, John C. Vickerman and David E. Sanders for insightful discussions.

References

[1] N.Winograd and B.J. Garrison, in: Ion spectroscopies for surface analysis, eds. A.W. Czanderna and D.M. Hercules (Plenum Press, New York, 1991) pp. 45–141.

[2] G.J. Leggett and J.C. Vickerman, Intern. J. Mass Spectrom. Ion. Processes 86 (1988) 169.
[3] J.R. Creighton and J.M. White, Surface Sci. 129 (1983) 327.
[4] K.M. Ogle and J.M. White, Surface Sci. 165 (1986) 234.
[5] K.M. Ogle, J.R. Creighton, S.A. Akhter and J.M. White, Surface Sci. 169 (1986) 246.
[6] M.P. Kaminsky, N. Winograd, G.L. Geoffroy and M.A. Vannice, J. Am. Chem. Soc. 108 (1986) 1315.
[7] B.H. Sakakini, I.A. Ransley, C.F. Oduoza and J.C. Vickerman, Surface Sci. 271 (1992) 227.
[8] D.E. Harrison Jr., CRC Crit. Rev. Solid State Mater. Sci. 14 (1988) 51.
[9] B.J. Garrison, Chem. Soc. Rev. 21 (1992) 155.
[10] B.J. Garrison, N. Winograd and D.E. Harrison Jr., J. Chem. Phys. 69 (1978) 1440.
[11] B.J. Garrison, N. Winograd, D.M. Deaven, C.T. Reimann, D.Y. Lo, T.A. Tombrello, D.E. Harrison Jr. and M.H. Shapiro, Phys. Rev. B 37 (1988) 7197.
[12] B.J. Garrison, J. Am. Chem. Soc. 102 (1980) 6553.
[13] B.J. Garrison, J. Am. Chem. Soc. 104 (1982) 6211.
[14] B.J. Garrison, Intern. J. Mass Spec. Ion. Phys. 53 (1983) 243.
[15] D.W. Moon, N. Winograd and B.J. Garrison, Chem. Phys. Letters 114 (1985) 237.
[16] D.W. Brenner, Phys. Rev. B 42 (1990) 9458.
[17] D.W. Brenner, J.A. Harrison, C.T. White and R.J. Colton, Thin Solid Films 206 (1991) 220.
[18] S.M. Foiles, M.I. Baskes and M.S. Daw, Phys. Rev. B 33 (1986) 7983.
[19] M.S. Daw and M.I. Baskes, Phys. Rev. B 29 (1984) 6443.
[20] M.S. Daw and M.I. Baskes, Phys. Rev. Letters 50 (1983) 1285.
[21] B.J. Garrison, N. Winograd, D.M. Deaven, C.T. Reimann, D.Y. Lo, T.A. Tombrello, D.E. Harrison Jr. and M.H. Shapiro, Phys. Rev. B 37 (1988) 7197.
[22] R.S. Taylor and B.J. Garrison, J. Am. Chem. Soc. 116 (1994) 4465.
[23] R.S. Taylor and B.J. Garrison, submitted for publication.
[24] R.S.Taylor, Ph.D. Thesis, Penn State University (1994).
[25] D.J. O'Connor and R.J. Macdonald, Radiat. Eff. 34 (1977) 247.
[26] A. Wucher and B.J. Garrison, Surface Sci. 260 (1992) 257.
[27] D.W. Brenner, D.H. Robertson, R.L. Carty, D. Srivastava and B.J. Garrison, MRS Symp. Proc. 278 (1992) 255.
[28] X. Chang, M. Perry, J. Peploski, D.L. Thompson and L.M. Raff, J. Chem. Phys. 99 (1993) 4748.
[29] J.A. Harrison, C.T. White, R.J. Colton and D.W. Brenner, Surface Sci. 271 (1992) 57.
[30] J.A. Harrison, C.T. White, R.J. Colton and D.W. Brenner, Phys. Rev. B 46 (1992) 9700.
[31] J.A. Harrison, C.T. White, R.J. Colton and D.W. Brenner, J. Phys. Chem. 97 (1993) 6573.
[32] J.A. Harrison, C.T. White, R.J. Colton and D.W. Brenner, MRS Bulletin 18 (1993) 50.
[33] U. Starke, A. Barbieri, N. Materer, M.A. Van Hove and G.A. Somorjai, Surface Sci. 286 (1993) 1, and references therein.
[34] E.A. Carter and B.E. Koel, Surface Sci. 226 (1990) 339.
[35] R.S. Taylor, C.L. Brummel, N. Winograd, B.J. Garrison and J.C. Vickerman, to be published.
[36] R.J. Koestner, J.C. Frost, P.C. Stair, M.A. Van Hove and G.A. Somorjai, Surface Sci. 116 (1982) 85.
[37] J.A. Blush, H. Clauberg, D.W. Kohn, D.W. Minsek, X. Zhang and P. Chen, Accounts Chem. Res. 25 (1992) 385.